JOURNAL OF SMOOTH MUSCLE RESEARCH

J. Smooth Muscle Res. 2014; 50: 18–28
Published online: April 26, 2014; doi: 10.1540/jsmr.50.18

Invited Review

The involvement of myosin regulatory light chain diphosphorylation in sustained vasoconstriction under pathophysiological conditions

Kosuke Takeya[1, 2], Xuemei Wang[3], Cindy Sutherland[2], Iris Kathol[2, 3], Kathy Loutzenhiser[3], Rodger D. Loutzenhiser[3] and Michael P. Walsh[2]

[1]*Department of Physiology, Asahikawa Medical College, Hokkaido, Japan*
[2]*Department of Biochemistry and Molecular Biology, University of Calgary, Alberta, Canada*
[3]*Department of Physiology and Pharmacology, University of Calgary, Alberta, Canada*

Submitted January 16, 2014; accepted in final form February 3, 2014

Abstract

Smooth muscle contraction is activated primarily by phosphorylation at Ser19 of the regulatory light chain subunits (LC_{20}) of myosin II, catalysed by Ca^{2+}/calmodulin-dependent myosin light chain kinase. Ca^{2+}-independent contraction can be induced by inhibition of myosin light chain phosphatase, which correlates with diphosphorylation of LC_{20} at Ser19 and Thr18, catalysed by integrin-linked kinase (ILK) and zipper-interacting protein kinase (ZIPK). LC_{20} diphosphorylation at Ser19 and Thr18 has been detected in mammalian vascular smooth muscle tissues in response to specific contractile stimuli (e.g. endothelin-1 stimulation of rat renal afferent arterioles) and in pathophysiological situations associated with hypercontractility (e.g. cerebral vasospasm following subarachnoid hemorrhage). Comparison of the effects of LC_{20} monophosphorylation at Ser19 and diphosphorylation at Ser19 and Thr18 on contraction and relaxation of Triton-skinned rat caudal arterial smooth muscle revealed that phosphorylation at Thr18 has no effect on steady-state force induced by Ser19 phosphorylation. On the other hand, the rates of dephosphorylation and relaxation are significantly slower following diphosphorylation at Thr18 and Ser19 compared to monophosphorylation at Ser19. We propose that this diphosphorylation mechanism underlies the prolonged contractile response of particular vascular smooth muscle tissues to specific stimuli, e.g. endothelin-1 stimulation of renal afferent arterioles, and the vasospastic behavior observed in pathological conditions such as cerebral vasospasm following subarachnoid hemorrhage and coronary arterial vasospasm. ILK and ZIPK may, therefore, be useful therapeutic targets for the treatment of such conditions.

Key words: smooth muscle, renal microcirculation, myosin phosphorylation, integrin-linked kinase, zipper-interacting protein kinase

Abbreviations used: $[Ca^{2+}]_i$, cytosolic free Ca^{2+} concentration; CaM, calmodulin; CPI-17, 17-kDa PKC-potentiated inhibitory protein of PP1; ILK, integrin-linked kinase; LC_{17}, 17-kDa light chain of myosin; LC_{20}, 20-kDa light chain of myosin; MLCK, myosin light chain kinase; MLCP, myosin light chain phosphatase; MYPT1, myosin-targeting subunit of MLCP; PKC, protein kinase C; ROK, Rho-associated kinase; ZIPK, zipper-interacting protein kinase.

Corresponding author: Michael P. Walsh, Ph.D., FRSC, Department of Biochemistry and Molecular Biology, Faculty of Medicine, University of Calgary, 3330 Hospital Drive N.W., Calgary, AB T2N 4N1, Canada
Phone: +1-403-220-3021 Fax: +1-403-270-2211 e-mail: walsh@ucalgary.ca

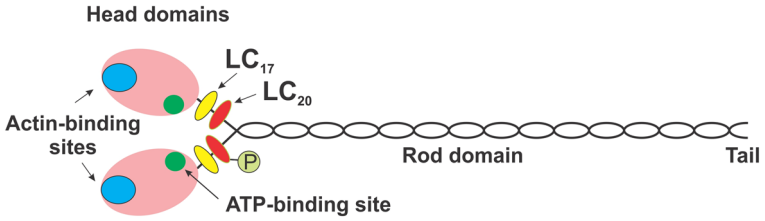

Fig. 1. Schematic representation of smooth muscle myosin II. Smooth muscle myosin II is a hexameric protein composed of two heavy chains (205 kDa each) and two pairs of light chains: the 17-kDa essential light chains (LC_{17}) and the 20-kDa regulatory light chains (LC_{20}). The *N*-termini of the heavy chains make up most of the head domains (pink) and the *C*-termini of the heavy chains account for the complete coiled-coil rod domain (which is responsible for assembly of myosin filaments) and the terminal unstructured tail (black). Each globular head includes an actin-binding site (blue) and an ATP-binding site (green). The light chains, LC_{17} (yellow) and LC_{20} (red), are associated with the neck region. "P" denotes phosphorylation of LC_{20}. This figure was originally published in IUBMB Life. Walsh MP. Vascular smooth muscle myosin light chain diphosphorylation: mechanism, function and pathological implications. 2011; 63(11): 987–1000. © John Wiley & Sons, Inc.

The central role of myosin regulatory light chain phosphorylation in the activation of smooth muscle contraction

Vascular smooth muscle contraction is activated by an increase in cytosolic free Ca^{2+} concentration ($[Ca^{2+}]_i$) as a result of Ca^{2+} entry from the extracellular space and/or Ca^{2+} release from intracellular stores, primarily the sarcoplasmic reticulum (1). Ca^{2+} diffuses to the contractile machinery where it binds to calmodulin (CaM) (2). The $(Ca^{2+})_4$-CaM complex induces a conformational change in myosin light chain kinase (MLCK), which involves removal of the autoinhibitory domain from the active site, thereby converting the kinase from an inactive to an active state (3). MLCK is physically bound through its *N*-terminus to actin filaments and, upon activation, phosphorylates nearby myosin molecules (4). Myosin II filaments are composed of hexameric myosin molecules, each consisting of two heavy chains and two pairs of light chains (17-kDa essential light chains (LC_{17}) and 20-kDa regulatory light chains (LC_{20})) located in the neck region of the myosin molecule (Fig. 1). Activated MLCK phosphorylates Ser19 of LC_{20} and this simple post-translational modification induces a conformational change that is transmitted to the myosin heads, resulting in actin interaction and a marked increase in the actin-activated MgATPase activity of myosin (5). The energy derived from the hydrolysis of ATP then drives cross-bridge cycling and the development of force or contraction of the muscle. Relaxation follows the removal of Ca^{2+} from the cytosol, primarily by CaATPases, which pump Ca^{2+} out of the cell and back into the sarcoplasmic reticulum (6). MLCK is inactivated as Ca^{2+} dissociates from CaM and the autoinhibitory domain of MLCK blocks the active site. Phosphorylated myosin is then dephosphorylated by myosin light chain phosphatase (MLCP), a type 1 protein serine/threonine phosphatase (7).

Ca^{2+} sensitization

MLCP is a trimeric phosphatase with a 38-kDa catalytic subunit (PP1cδ), a 130-kDa regulatory subunit (MYPT1) and a 21-kDa subunit of uncertain function. MYPT1 targets the phosphatase holoenzyme to myosin and enhances its activity. MLCP is inhibited by both protein kinase C (PKC) and RhoA/Rho-associated kinase

(ROK) pathways. Phosphorylation of the cytosolic phosphatase inhibitory protein of 17-kDa (CPI-17) at Thr38 by PKC converts CPI-17 to a potent inhibitor of MLCP, which is achieved by direct interaction of phosphorylated CPI-17 with PP1cδ (8). ROK is also capable of phosphorylating CPI-17 at Thr38 (9). In addition, and apparently of greater physiological significance, ROK phosphorylates MYPT1 to induce inhibition of MLCP activity. ROK phosphorylates MYPT1 at Thr697 and Thr855 (rat numbering) *in vitro* and both phosphorylation events result in phosphatase inhibition (10). However, it appears that ROK predominantly phosphorylates Thr855 in intact tissues (11). Activation of PKC and ROK pathways, therefore, can result in decreased MLCP activity, resulting in an increase in the ratio of MLCK : MLCP activity and an increase in force. Since ROK and novel PKC isoforms are Ca^{2+}-independent, this results in Ca^{2+} sensitization of contraction, i.e. an increase in force without an increase in $[Ca^{2+}]_i$.

Myosin regulatory light chain diphosphorylation

The possibility that LC_{20} may also be phosphorylated at Thr18 was originally demonstrated *in vitro* when it was shown that high concentrations of MLCK phosphorylate Thr18 in addition to Ser19 (12). It is clear, however, that MLCK does not phosphorylate Thr18 of LC_{20} in intact smooth muscle tissues, and most contractile stimuli are associated with LC_{20} phosphorylation exclusively at Ser19, which can be attributed to MLCK (13). Interest in Thr18 phosphorylation was revived, however, when it was shown that treatment of smooth muscle tissues with membrane-permeant phosphatase inhibitors (such as calyculin-A) induced Ca^{2+}-independent contractions that correlated with diphosphorylation of LC_{20} at Thr18 and Ser19 (14). Two Ca^{2+}-independent kinases (integrin-linked kinase (ILK) and zipper-interacting protein kinase (ZIPK)) were shown to be the most likely kinases responsible for LC_{20} diphosphorylation (15–17).

Evidence of myosin regulatory light chain diphosphorylation in intact smooth muscle tissues

Phosphorylation of LC_{20} at Thr18 and Ser19 has been observed in several smooth muscle tissues, e.g. bovine tracheal smooth muscle in response to neural stimulation or carbachol (18, 19), rabbit thoracic aorta treated with prostaglandin-$F_{2\alpha}$ (20, 21) and renal afferent arterioles stimulated with endothelin-1 (22). LC_{20} diphosphorylation has frequently been associated with pathophysiological conditions involving hypercontractility, including cerebral vasospasm (23), coronary (24, 25) and femoral arterial vasospasm (26), intimal hyperplasia (27) and hypertension (28).

The functional effects of diphosphorylation of myosin regulatory light chains

Early studies comparing the properties of smooth muscle myosin phosphorylated at Ser19 (by low concentrations of MLCK) and at both Thr18 and Ser19 (by high concentrations of MLCK) indicated that the additional phosphorylation at Thr18 increased the actomyosin MgATPase activity some two- to three-fold (12, 29–31). However, the velocity of movement of myosin-coated beads along actin cables (32) or of actin filaments over immobilized myosin in the *in vitro* motility assay (31) was similar whether LC_{20} was phosphorylated at Ser19 alone or at both Thr18 and Ser19. We recently addressed the hypothesis that phosphorylation at Thr18 may enhance the level of steady-state force achieved with Ser19 phosphorylation (13). To test this hypothesis, we used

Triton-skinned rat caudal arterial smooth muscle strips. The objective was to achieve stoichiometric phosphorylation of LC_{20} at Ser19, then elicit phosphorylation at Thr18 and observe whether or not there was a further increase in steady-state force. The challenge was to achieve stoichiometric phosphorylation at Ser19 since this cannot be done in intact tissue due to the competing actions of MLCK and MLCP, which results in stable phosphorylation of LC_{20} at steady-state of ≤ 0.5 mol P_i/mol LC_{20}. Furthermore, this problem cannot be overcome by inhibition of phosphatase activity since phosphatase inhibitors such as calyculin-A and okadaic acid unmask the basal activities of ILK and ZIPK, which phosphorylate both Thr18 and Ser19 of LC_{20}. We took advantage of the fact that protein kinases generally, including MLCK, can utilize adenosine 5′-*O*-(3-thiotriphosphate) (ATPγS) as a substrate to thiophosphorylate their protein substrates (33), but the thiophosphorylated protein (LC_{20} in this case) is a very poor phosphatase substrate (34). It was necessary to use Triton-skinned tissue for this experiment since the plasma membrane is impermeant to ATPγS. Fig. 2 shows the experimental protocol and corresponding force measurements (Fig. 2A) and analysis of LC_{20} (thio)phosphorylation by Phos-tag SDS-PAGE (see below for a description of this technique, which enables the separation of unphosphorylated and phosphorylated forms of LC_{20}) (Fig. 2B). At resting tension (pCa 9), LC_{20} is unphosphorylated (lanes 1 and 8, Fig. 2B). A control contraction was elicited by increasing $[Ca^{2+}]$ to pCa 4.5 in the presence of ATP and relaxation followed removal of Ca^{2+} (Fig. 2A). When basal force was restored, the tissue was washed several times in pCa 9 solution without ATP to remove all ATP, following which ATPγS was added at pCa 4.5 to elicit close-to-stoichiometric LC_{20} thiophosphorylation (Fig. 2B, lanes 2 and 3). Contraction did not occur under these conditions since ATPγS is not hydrolysed by the actin-activated myosin MgATPase and, therefore, ATPγS cannot support cross-bridge cycling (35–37). Following LC_{20} thiophosphorylation, ATPγS was washed out by several washes with pCa 9 solution (Fig. 2A). This was accompanied by very little dethiophosphorylation of LC_{20} (Fig. 2B, lane 4). ATP was then added at pCa 9, whereupon the tissue contracted rapidly due to the fact that LC_{20} was previously thiophosphorylated. Again there was very little dethiophosphorylation during this treatment (Fig. 2B, lane 5). The level of force achieved during this treatment was comparable to that elicited initially by addition of ATP at pCa 4.5 (Fig. 2A). Finally, the phosphatase inhibitor microcystin was added at pCa 9 in the presence of ATP, whereupon Ser19-thiophosphorylated LC_{20} was phosphorylated at Thr18 (1S1P in lanes 6 and 7 of Fig. 2B). Small amounts of monophosphorylated (1P) and diphosphorylated (2P) LC_{20} were also detected due to the presence (Fig. 2B, lane 5) of a small amount of unphosphorylated LC_{20} prior to the addition of microcystin. Fig. 2B, lane 9 shows a control Triton-skinned tissue treated with microcystin and ATP at pCa 9 to indicate the migration of unphosphorylated (0P), monophosphorylated (1P) and diphosphorylated (2P) LC_{20}, as previously established (13). The key finding from this experiment was that phosphorylation of LC_{20} at Thr18 on top of close-to-stoichiometric thiophosphorylation of LC_{20} at Ser19 did not elicit an increase in force.

We next addressed the hypothesis that phosphorylation of LC_{20} at both Thr18 and Ser19 reduces the rate of dephosphorylation and relaxation compared to phosphorylation at Ser19 alone. To test this hypothesis, LC_{20} was phosphorylated at Ser19 only or at both Thr18 and Ser19 to comparable stoichiometry. This was achieved by treatment of Triton-skinned rat caudal arterial smooth muscle strips with ATP at pCa 4.5 (for monophosphorylation at Ser19) or with ATP and the phosphatase inhibitor okadaic acid at pCa 9 (for diphosphorylation at Thr18 and Ser19). The time-courses of dephosphorylation and relaxation were then followed to determine if there was a reduction in the rates of dephosphorylation and relaxation when LC_{20} was diphosphorylated at Thr18 and Ser19 compared to monophosphorylated at Ser19. As shown in Fig. 3A and C, both treatments induced LC_{20} phosphorylation to ~ 0.5 mol P_i/mol LC_{20}. At pCa 4.5, this was exclusively Ser19 phosphorylation, whereas in response to okadaic acid at pCa 9, phosphorylation occurred at both Thr18 and Ser19 (Fig. 3C). Comparison of the time-courses of dephosphorylation (Fig. 3A and C) and relaxation (Fig. 3B) clearly shows

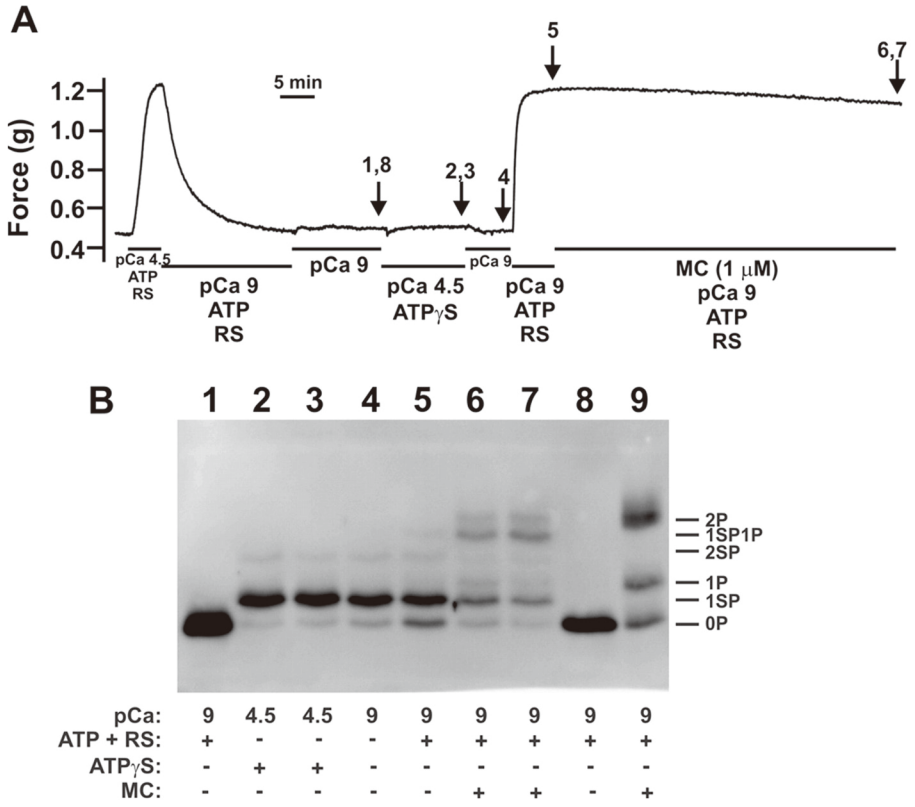

Fig. 2. Stoichiometric thiophosphorylation of LC_{20} at Ser19 in Triton-skinned rat caudal arterial smooth muscle. (A) The viability of Triton-skinned rat caudal arterial smooth muscle strips was initially verified by transfer from relaxing solution (pCa 9) to high [Ca^{2+}] (pCa 4.5) solution containing ATP and an ATP regenerating system (RS), which induced a contractile response. Tissues were then relaxed by 3 washes in pCa 9 solution containing ATP and RS. ATP was then removed by 6 washes in pCa 9 solution without ATP or RS. Tissues were then incubated in pCa 4.5 solution containing ATPγS (4 mM) in the absence of ATP and RS. Excess ATPγS was then removed by washing twice with pCa 9 solution without ATP or RS. Contraction was evoked by transfer to pCa 9 solution containing ATP and RS. Once steady-state force was established, microcystin (1 μM) was added in pCa 9 solution containing ATP and RS. Tissues were harvested at the indicated times during this protocol for Phos-tag SDS-PAGE and western blotting with anti-pan LC_{20} (B), as shown by the arrows in (A) (the numbers correspond to the lanes in (B)): (i) lanes 1 and 8, tissue incubated at pCa 9 showing exclusively unphosphorylated LC_{20}; (ii) lanes 2 and 3, pCa 4.5 + ATPγS in the absence of ATP and RS; (iii) lane 4, pCa 9 in the absence of ATP and RS following thiophosphorylation; (iv) lane 5, at the plateau of force development following transfer to pCa 9 solution containing ATP and RS; (v) lanes 6 and 7, following treatment with microcystin at pCa 9 in the presence of ATP and RS. An additional control is included in lane 9: Triton-skinned tissue treated with microcystin at pCa 9 for 60 min to identify unphosphorylated (0P), monophosphorylated (1P), and diphosphorylated (2P) LC_{20} bands. Thiophosphorylated forms of LC_{20} are indicated as follows: 1SP, monothiophosphorylated LC_{20}; 2SP, dithiophosphorylated LC_{20}; 1SP1P, LC_{20} thiophosphorylated at one site and phosphorylated at the other. Data are representative of 8 independent experiments. This research was originally published in the Journal of Biological Chemistry. Sutherland C, Walsh MP. Myosin regulatory light chain diphosphorylation slows relaxation of arterial smooth muscle. 2012; 287(29): 24064–76. © the American Society for Biochemistry and Molecular Biology.

that both dephosphorylation and relaxation rates were significantly slower when LC_{20} was diphosphorylated at Thr18 and Ser19 compared to monophosphorylated at Ser19. This finding suggests a functional effect of LC_{20} diphosphorylation and raises the possibility that pathological situations of hypercontractility may result from impaired relaxation due to this dephosphorylation event. MLCP has been shown to dephosphorylate Thr18 in

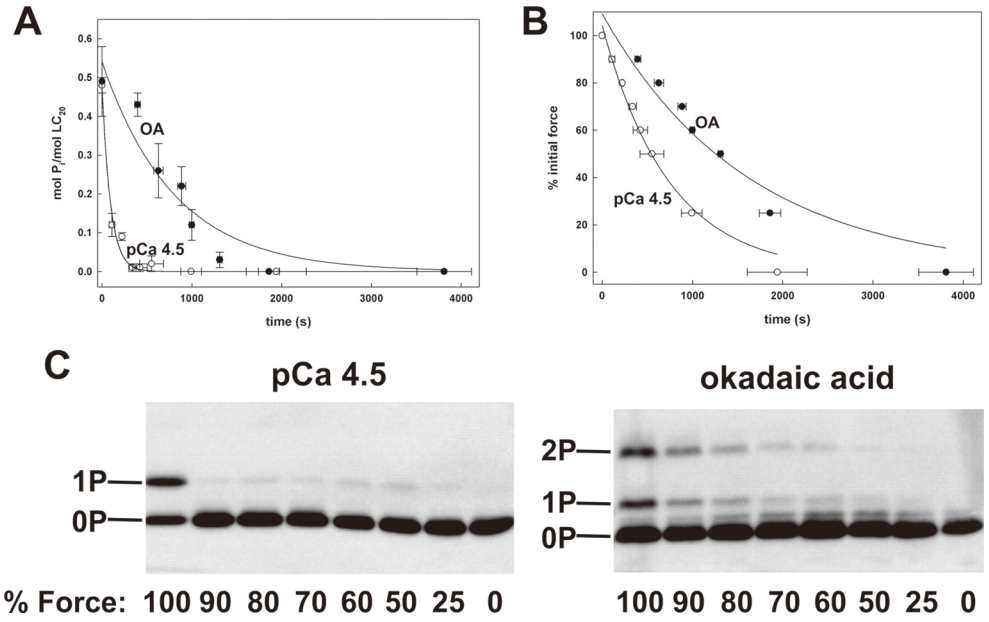

Fig. 3. Comparison of the time courses of relaxation and LC_{20} dephosphorylation in Triton-skinned rat caudal arterial smooth muscle following contraction with Ca^{2+} or okadaic acid in the absence of Ca^{2+}. Triton-skinned tissues that had been contracted with Ca^{2+} (open circles) or okadaic acid (20 μM) at pCa 9 (closed circles) were transferred to pCa 9 solution and the time courses of dephosphorylation (A) and relaxation (B) were followed. Tissues were harvested at 10, 20, 30, 40, 50, 75, and 100% relaxation and LC_{20} phosphorylation levels were quantified by Phos-tag SDS-PAGE and western blotting with anti-pan LC_{20}. Values represent the mean ± S.E. (n = 5). Representative western blots are shown in (C). This research was originally published in the Journal of Biological Chemistry. Sutherland C, Walsh MP. Myosin regulatory light chain diphosphorylation slows relaxation of arterial smooth muscle. 2012; 287(29): 24064–76. © the American Society for Biochemistry and Molecular Biology.

addition to Ser19 (38) suggesting that the same phosphatase dephosphorylates mono- and diphosphorylated LC_{20} *in situ*.

The renal microvasculature

Fig. 4 provides a schematic representation of the renal microcirculation, which consists of the afferent arteriole conveying blood from the interlobular artery to the glomerular capillaries where it is filtered prior to returning to the systemic circulation via the efferent arteriole. The afferent arteriole plays a key role in regulating glomerular inflow resistance and must be able to respond very rapidly to sudden changes in systemic blood pressure in order to protect the fragile glomeruli from pressure-induced damage (39). Angiotensin II (Ang II) is a renal-selective vasoconstrictor that contributes to renal vascular resistance under normal physiological conditions and thereby plays an important role in modulating renal hemodynamics (40). Endothelin-1 (ET-1), on the other hand, is a renal vasoconstrictor that does not contribute to renal vascular resistance under normal physiological conditions, but is implicated in abnormal renal vasoconstriction and reduced glomerular filtration in pathological states such as diabetes and chronic kidney disease (41–47).

Based on our studies of the effects of LC_{20} diphosphorylation described above, we developed a hypothesis that pathological situations of hypercontractility may result from impaired relaxation due to diphosphorylation

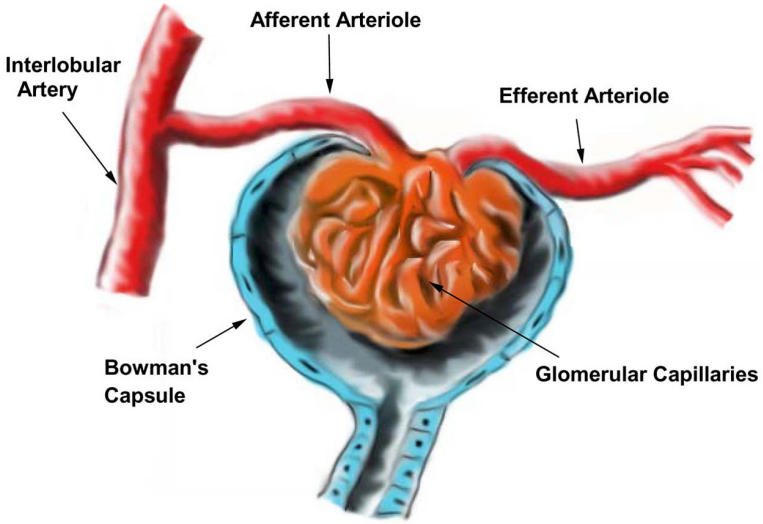

Fig. 4. Schematic diagram illustrating the anatomical relationship of the afferent arteriole, glomerulus, and the efferent arteriole**.** The afferent arteriole controls the glomerular inflow resistance. This vessel must constrict rapidly in response to fluctuations in blood pressure to prevent pressure elevations from being transmitted to the downstream glomerular capillaries. The efferent arteriole originates at the glomerular capillaries and regulates glomerular outflow resistance. When renal perfusion pressure is compromised, a sustained increase in efferent arteriolar tone maintains adequate filtration pressure within the upstream glomerular capillaries, thereby preserving renal function. This figure was reproduced from ref. (52) with permission.

of LC_{20} at Thr18 and Ser19. We have tested this hypothesis by studying the effects of two contractile stimuli, one physiological (Ang II) and one pathophysiological (ET-1), on renal afferent arteriolar constriction and LC_{20} phosphorylation. We compared the patterns of phosphorylation of LC_{20} in the afferent arteriole to determine whether or not LC_{20} diphosphorylation is associated with the pathophysiological stimulus ET-1 and not the physiological stimulus Ang II. This proved to be a challenging proposition due largely to the very small size of the afferent arteriole: a single afferent arteriole has a diameter of 15–20 μm, contains < 100 smooth muscle cells and is ~ $1/10^{th}$ the size of a human eyelash. This necessitated developing a technique to isolate individual afferent arterioles and enhance the sensitivity of detection and quantification of LC_{20} phosphorylation. Perfusion of the renal artery with molten agarose followed by cooling to solidify the agarose enabled dissection and recovery of intact afferent arterioles (48). Phos-tag SDS-PAGE (49) proved to be a suitable technique for rapid and efficient separation of unphosphorylated and phosphorylated forms of LC_{20} (50). In this technique, tissue proteins are separated in Laemmli SDS gels in which a phosphate-binding ligand (Phos-tag reagent) is immobilized in the running gel. In the presence of Mn^{2+} ions, the migration of proteins containing phosphorylated serine, threonine and/or tyrosine residues is retarded due to binding to the ligand. The higher the stoichiometry of phosphorylation, the slower the migration rate through the gel. The protein of interest (LC_{20} in this instance) is then detected by western blotting with an antibody that recognizes all forms of the protein, phosphorylated and unphosphorylated. The effectiveness of the separation of the various LC_{20} species by Phos-tag SDS-PAGE can be clearly seen in Figs. 2B and 3C. Quantification of the different LC_{20} species by densitometric scanning enables determination of the stoichiometry of phosphorylation, and the individual phosphorylation sites can be identified by using phosphorylation site-specific antibodies in parallel western blotting experiments. We were able to increase the sensitivity of detection of LC_{20} > 4,000-fold over existing methods (50). This was achieved

by: (i) the use of biotinylated secondary antibodies in conjunction with streptavidin-conjugated horseradish peroxidase, combined with enhanced chemiluminescence detection of LC_{20} species, (ii) fixing the LC_{20} on the PVDF membrane by treatment with glutaraldehyde, and (iii) incorporating CanGetSignal® (Toyobo, Japan) into the protocol. Utilization of a minimum number of steps in the protocol with the least possible number of sample transfers maximized LC_{20} yield. The limit of detection of LC_{20} was thereby increased from ~ 200 fmol (4 ng) to ~ 0.05 fmol (1 pg); we estimate that a single afferent arteriole contains ~ 2.5 fmol (50 pg) of LC_{20}.

Using this approach, we succeeded in quantifying LC_{20} phosphorylation levels in single isolated afferent arterioles and observed that Ang II induced exclusively monophosphorylation of LC_{20} whereas ET-1 induced diphosphorylation, both in a time- and concentration-dependent manner (22). ET-1-induced diphosphorylation was confirmed to occur at Thr18 and Ser19 using phosphorylation site-specific antibodies. ET-1-induced LC_{20} diphosphorylation was confirmed by the proximity ligation assay (51). Furthermore, afferent arteriolar vasodilation (relaxation) occurred more slowly following washout of ET-1 than Ang II (22). These findings are, therefore, consistent with the hypothesis that pathophysiological signals such as ET-1 that are associated with prolonged vasoconstrictor responses involve LC_{20} diphosphorylation, whereas physiological signals such as Ang II induce LC_{20} phosphorylation exclusively at Ser19. The additional phosphorylation at Thr18 induced by ET-1 is, therefore, proposed to account, at least in part, for the sustained contractile response of the afferent arteriole to ET-1 compared to Ang II.

Conclusions

LC_{20} is phosphorylated at Thr18 and Ser19 in a Ca^{2+}-independent manner by ILK and/or ZIPK, which are associated with the contractile machinery in vascular smooth muscle. This occurs in concert with inhibition of MLCP by ROK-catalysed phosphorylation of MYPT1, the regulatory and targeting subunit of the phosphatase. Diphosphorylation of LC_{20} occurs in response to ET-1 (pathological stimulus) but not Ang II (physiological stimulus) in renal afferent arterioles, and diphosphorylation of LC_{20} is associated with decreased rates of LC_{20} dephosphorylation and relaxation. ILK and ZIPK are, therefore, potential therapeutic targets for the treatment of diseases associated with hypercontractility, such as hypertension, cerebral vasospasm following subarachnoid hemorrhage, coronary arterial vasospasm, intimal hyperplasia, acute renal insufficiency and chronic kidney disease.

Acknowledgments

The work described in this review was supported by grant MOP-93806 to R.L. and M.P.W. and grant MOP-111262 to M.P.W. from the Canadian Institutes of Health Research. R.L. was an Alberta Innovates - Health Solutions (AI-HS) Scientist. M.P.W. is an AI-HS Scientist and Canada Research Chair (Tier 1) in Vascular Smooth Muscle Research.

Conflict of interest

The authors declare that they have no conflict of interest.

References

1. Somlyo AP, Somlyo AV. Ca^{2+} sensitivity of smooth muscle and nonmuscle myosin II: modulated by G proteins, kinases and myosin phosphatase. Physiol Rev. 2003; 83(4): 1325–58.
2. Wilson DP, Sutherland C, Walsh MP. Ca^{2+} activation of smooth muscle contraction: evidence for the involvement of calmodulin that is bound to the triton-insoluble fraction even in the absence of Ca^{2+}. J Biol Chem. 2002; 277(3): 2186-92.
3. Allen BG, Walsh MP. The biochemical basis of the regulation of smooth-muscle contraction. Trends Biochem Sci. 1994; 19(9): 362–8.
4. Kamm KE, Stull JT. Dedicated myosin light chain kinases with diverse cellular functions. J Biol Chem. 2001; 276(7): 4527–30.
5. Walsh MP. Calcium-dependent mechanisms of regulation of smooth muscle contraction. Biochem Cell Biol. 1991; 69(12): 771–800.
6. Raeymaekers L, Wuytack F. Ca^{2+} pumps in smooth muscle cells. J Muscle Res Cell Motil. 1993; 14(2): 141–57.
7. Hartshorne DJ, Ito M, Erdödi F. Role of protein phosphatase type 1 in contractile functions: Myosin phosphatase. J Biol Chem. 2004; 279(36): 37211–4.
8. Eto M. Regulation of cellular protein phosphatase-1 (PP1) by phosphorylation of the CPI-17 family, C-kinase-activated PP1 inhibitors. J Biol Chem. 2009; 284(51): 35273–7.
9. Koyama M, Ito M, Feng J, Seko T, Shiraki K, Takase K, Hartshorne DJ, Nakano T. Phosphorylation of CPI-17, an inhibitory phosphoprotein of smooth muscle myosin phosphatase, by Rho-kinase. FEBS Lett. 2000; 475(3): 197–200.
10. Murányi A, Derkach D, Erdödi F, Kiss A, Ito M, Hartshorne DJ. Phosphorylation of Thr695 and Thr850 on the myosin phosphatase target subunit: inhibitory effects and occurrence in A7r5 cells. FEBS Lett. 2005; 579(29): 6611–5.
11. Borysova L, Shabir S, Walsh MP, Burdyga T. The importance of Rho-associated kinase-induced Ca^{2+} sensitization as a component of electromechanical and pharmacomechanical coupling in rat ureteric smooth muscle. Cell Calcium. 2011; 50(4): 393–405**.**
12. Ikebe M, Hartshorne DJ. Phosphorylation of smooth muscle myosin at two distinct sites by myosin light chain kinase. J Biol Chem. 1985; 260(18): 10027–31.
13. Sutherland C, Walsh MP. Myosin regulatory light chain diphosphorylation slows relaxation of arterial smooth muscle. J Biol Chem. 2012; 287(29): 24064–76.
14. Weber LP, Van Lierop JE, Walsh MP. Ca^{2+}-independent phosphorylation of myosin in rat caudal artery and chicken gizzard myofilaments. J Physiol. 1999; 516(3): 805–24.
15. Deng JT, Van Lierop JE, Sutherland C, Walsh MP. Ca^{2+}-independent smooth muscle contraction. a novel function for integrin-linked kinase. J Biol Chem. 2001; 276(19): 16365–73.
16. Niiro N, Ikebe M. Zipper-interacting protein kinase induces Ca^{2+}-free smooth muscle contraction via myosin light chain phosphorylation. J Biol Chem. 2001; 276(31): 29567–74.
17. Moffat LD, Brown SB, Grassie ME, Ulke-Lemée A, Williamson LM, Walsh MP, MacDonald JA. Chemical genetics of zipper-interacting protein kinase reveal myosin light chain as a *bona fide* substrate in permeabilized arterial smooth muscle. J Biol Chem. 2011; 286(42): 36978–91.
18. Miller-Hance WC, Miller JR, Wells JN, Stull JT, Kamm KE. Biochemical events associated with activation of smooth muscle contraction. J Biol Chem. 1988; 263(28): 13979–82.
19. Colburn JC, Michnoff CH, Hsu LC, Slaughter CA, Kamm KE, Stull JT. Sites phosphorylated in myosin light chain in contracting smooth muscle. J Biol Chem. 1988; 263(35): 19166–73.
20. Seto M, Sasaki Y, Sasaki Y. Stimulus-specific patterns of myosin light chain phosphorylation in smooth

muscle of rabbit thoracic aorta. Pflügers Arch. 1990; 415(4): 484–9.

21. Seto M, Sasaki Y, Sasaki Y, Hidaka H. Effect of HA1077, protein kinase inhibitor, on myosin phosphorylation and tension in smooth muscle. Eur J Pharmacol. 1991; 195(2): 267–72.
22. Takeya K, Wang X, Kathol I, Loutzenhiser R, Walsh MP. Endothelin-1 induces sustained constriction of the rat renal afferent arteriole via diphosphorylation of the myosin regulatory light chains. J Physiol Sci. 2013; 63(Suppl 1): S275.
23. Obara K, Nishizawa S, Koide M, Nozawa K, Mitate A, Ishikawa T, Nakayama K. Interactive role of protein kinase C-δ with Rho kinase in the development of cerebral vasospasm in a canine two-hemorrhage model. J Vasc Res. 2005; 42(1): 67–76.
24. Katsumata N, Shimokawa H, Seto M, Kozai T, Yamawaki T, Kuwata K, Egashira K, Ikegaki I, Asano T, Sasaki Y, Takeshita A. Enhanced myosin light chain phosphorylations as a central mechanism for coronary artery spasm in a swine model with interleukin-1β. Circulation. 1997; 96(12): 4357–63.
25. Shimokawa H, Seto M, Katsumata N, Amano M, Kozai T, Yamawaki T, Kuwata K, Kandabashi T, Egashira K, Ikegaki I, Asano T, Kaibuchi K, Takeshita A. Rho kinase-mediated pathway induces enhanced myosin light chain phosphorylations in a swine model of coronary artery spasm. Cardiovasc Res. 1999; 43(4): 1029–39.
26. Harada T, Seto M, Sasaki Y, London S, Luo Z, Mayberg M. The time course of myosin light-chain phosphorylation in blood-induced vasospasm. Neurosurgery. 1995; 36(6): 1178–82.
27. Seto M, Yano K, Sasaki Y, Azuma H. Intimal hyperplasia enhances myosin phosphorylation in rabbit carotid artery. Exp Mol Pathol. 1993; 58(1): 1–13.
28. Cho YE, Ahn DS, Morgan KG, Lee YH. Enhanced contractility and myosin phosphorylation induced by Ca^{2+}-independent MLCK activity in hypertensive rats. Cardiovasc Res. 2011; 91(1): 162–70.
29. Tanaka T, Sobue K, Owada MK, Hakura A. Linear relationship between diphosphorylation of 20 kDa light chain of gizzard myosin and the actin-activated myosin ATPase activity. Biochem Biophys Res Commun. 1985; 131(2): 987–93.
30. Ikebe M, Koretz J, Hartshorne DJ. Effects of phosphorylation of light chain residues threonine 18 and serine 19 on the properties and conformation of smooth muscle myosin. J Biol Chem. 1988; 263(13): 6432–7.
31. Bresnick AR, Wolff-Long VL, Baumann O, Pollard TD. Phosphorylation on threonine-18 of the regulatory light chain dissociates the ATPase and motor properties of smooth muscle myosin II. Biochemistry. 1995; 34(39): 12576–83.
32. Umemoto S, Bengur AR, Sellers JR. Effect of multiple phosphorylations of smooth muscle and cytoplasmic myosins on movement in an *in vitro* motility assay. J Biol Chem. 1989; 264(3): 1431–6.
33. Sherry JMF, Górecka A, Aksoy MO, Dabrowska R, Hartshorne DJ. Roles of calcium and phosphorylation in the regulation of the activity of gizzard myosin. Biochemistry. 1978; 17(21): 4411–8.
34. Gratecos D, Fischer EH. Adenosine 5′-*O*-(3-thiotriphosphate) in the control of phosphorylase activity. Biochem Biophys Res Commun. 1974; 58(4): 960–7.
35. Cassidy P, Hoar PE, Kerrick WGL. Irreversible thiophosphorylation and activation of tension in functionally skinned rabbit ileum strips by [35S]ATPγS. J Biol Chem. 1979; 254(21): 11148–53.
36. Walsh MP, Bridenbaugh R, Hartshorne DJ, Kerrick WGL. Phosphorylation-dependent activated tension in skinned gizzard muscle fibers in the absence of Ca^{2+}. J Biol Chem. 1982; 257(11): 5987–90.
37. Walsh MP, Bridenbaugh R, Kerrick WGL, Hartshorne DJ. Gizzard Ca^{2+}-independent myosin light chain kinase. Evidence in favor of the phosphorylation theory. Fed Proc. 1983; 42(1): 45–50.
38. Feng J, Ito M, Nishikawa M, Okinaka T, Isaka N, Hartshorne DJ, Nakano T. Dephosphorylation of distinct sites on the 20 kDa myosin light chain by smooth muscle myosin phosphatase. FEBS Lett. 1999; 448(1): 101–4.
39. Loutzenhiser R, Griffin K, Williamson G, Bidani A. Renal autoregulation: new perspectives regarding

protective and regulatory roles of the underlying mechanisms. Am J Physiol. 2006; 290(5): R1153–67.

40. Edwards RM, Aiyar N. Angiotensin II receptor subtypes in the kidney. J Am Soc Nephrol. 1993; 3(10): 1643–52.
41. Gómez-Garre D, Largo R, Liu XH, Gutierrez S, López-Armada MJ, Palacios I, Egido J. An orally active ET_A/ET_B receptor antagonist ameliorates proteinuria and glomerular lesions in rats with proliferative nephritis. Kidney Int. 1996; 50(3): 962–72.
42. Orth SR, Esslinger JP, Amann K, Schwarz U, Raschack M, Ritz E. Nephroprotection of an ET_A-receptor blocker (LU 135252) in salt-loaded uninephrectomized stroke-prone spontaneously hypertensive rats. Hypertension. 1998; 31(4): 995–1001.
43. Wilhelm SM, Stowe NT, Robinson AV, Schulak JA. The use of the endothelin receptor antagonist, tezosentan, before and after renal ischemia protects renal function. Transplantation. 2001; 71(2): 211–6.
44. Kon V, Yoshioka T, Fogo A, Ichikawa I. Glomerular actions of endothelin *in vivo*. J Clin Invest. 1989; 83(5): 1762–7.
45. Loutzenhiser R, Epstein M, Hayashi K, Horton C. Direct visualization of effects of endothelin on the renal microvasculature. Am J Physiol. 1990; 258(1 Pt2): F61–8.
46. Claria J, Jimenez W, La Villa G, Asbert M, Castro A, Llibre JL, Arroyo V, Rivera F. Effects of endothelin on renal haemodynamics and segmental sodium handling in conscious rats. Acta Physiol Scand. 1991; 141(3): 305–8.
47. Harris PJ, Zhuo J, Mendelsohn FA, Skinner SL. Haemodynamic and renal tubular effects of low doses of endothelin in anaesthetized rats. J Physiol. 1991; 433(1): 25–39.
48. Loutzenhiser K, Loutzenhiser R. Angiotensin II-induced Ca^{2+} influx in renal afferent and efferent arterioles: differing roles of voltage-gated and store-operated Ca^{2+} entry. Circ Res. 2000; 87(7): 551–7.
49. Kinoshita E, Kinoshita-Kikuta E, Takiyama K, Koike T. Phosphate-binding tag, a new tool to visualize phosphorylated proteins. Mol Cell Proteomics. 2006; 5(4): 749–57.
50. Takeya K, Loutzenhiser K, Shiraishi M, Loutzenhiser R, Walsh MP. A highly sensitive technique to measure myosin regulatory light chain phosphorylation. The first quantification in renal arterioles. Am J Physiol. 2008; 294(6): F1487–92.
51. Söderberg O, Gullberg M, Jarvius M, Ridderstråle K, Leuchowius KJ, Jarvius J, Wester K, Hydbring P, Bahram F, Larsson LG, Landegren U. Direct observation of individual endogenous protein complexes *in situ* by proximity ligation. Nat Methods. 2006; 3(12): 995–1000.
52. Shiraishi M, Wang X, Walsh MP, Kargacin G, Loutzenhiser K, Louzenhiser R. Myosin heavy chain expression in renal afferent and efferent arterioles: relationship to contractile kinetics and function. FASEB J. 2003; 17(15): 2284–6.